ELSEVIER

Journal of Structural Geology 28 (2006) 1051–1066

JOURNAL OF STRUCTURAL GEOLOGY

www.elsevier.com/locate/jsg

Favoured states of palaeostress in the Earth's crust: evidence from fault-slip data

Richard J. Lisle [a,*], Tobore O. Orife [b], Luis Arlegui [c], Carlos Liesa [c], Deepak C. Srivastava [d]

[a] *School of Earth, Ocean and Planetary Sciences, Cardiff University, Cardiff CF10 3YE, Wales, UK*
[b] *BG Group, 100 Thames Valley Park Drive, Reading RG6 1PT, UK*
[c] *Departamento de Geología, Universidad de Zaragoza, Spain*
[d] *Department of Earth Sciences, Indian Institute of Technology, Roorkee 247667, India*

Abstract

In a major survey of published palaeostress estimates obtained by the use of fault-slip data, over 2000 stress tensors from shallow crustal levels have been compiled. The results are derived from regions where deformation is dominated by brittle processes, and consist of incomplete stress tensors in which the orientations of the principal stresses ($\sigma_1 \geqq \sigma_2 \geqq \sigma_3$) are known, together with the stress ratio, $\Phi = (\sigma_2 - \sigma_3)/(\sigma_1 - \sigma_3)$.

The orientations of the stress axes display a preferred orientation, with a tendency for one of the axes to be vertical. This accords with Anderson's assumed 'standard state' stress configuration near to the Earth's free surface. Although the tendency is strong, there are frequent deviations from the arrangement; in 25% of cases the steepest stress axis deviates by more than 25° from the vertical. In undertaking studies of palaeostress it would be therefore unwise to use methods that assume a priori one vertical stress axis unless previous local results indicate this to be the case. Normal, strike-slip and thrust stress arrangements (with σ_1, σ_2 and σ_3 as the steepest stress, respectively) occur in the database with frequencies approximately in the ratio 2:2:1.

In the compiled results, the raw stress ratios, Φ, which have a theoretical range from 0 to 1, show a lack of very high values and, to a lesser extent, very low values. This suggests that triaxial stress states are more common than axial compression deviatoric stress and axial tension deviatoric stress. However, this relative abundance of triaxial stress states is considered to be a natural feature of a uniform distribution of stress tensors. In addition, there is a marked bias in the collated ratios towards values less than 0.5 and this is expressed by an overall mean Φ of 0.39. Several possible explanations for the distribution of stress ratios are discussed. These explanations are related to the tendency for tectonic deformation to be of plane strain type coupled with volume change and to the fact that gravitational loading makes an important contribution to the state of stress in the crust.

Keywords: Faults; Stress survey; Slip; Stress ratio; Poisson's ratio

1. Introduction

Stress analysis from fault-slip data has developed over the last 25 years into a major sub-discipline of structural geology. Following the suggestion by Wallace (1951) and Bott (1959) that the observed slip direction on a fault surface can be used as an indicator of the resolved shear stress direction, a methodology has been developed for estimating palaeostress tensors from collections of data consisting of fault plane orientations and their associated slip lineations. The application of these methods to regions of brittle deformation at high crustal levels where strain accumulation has been dominantly the result of faulting has yielded an abundance of palaeostress results.

Studies of palaeostress have helped elucidate regional problems of crustal dynamics (e.g. Bergerat, 1987; Mercier et al., 1987) but in this paper we examine such results from a global perspective by compiling the numerous published results and examining these statistically. This analysis allows us to make general inferences about the nature of ancient stress states at shallow crustal levels in faulting-dominated regimes. The stress estimates discussed here relate to the stresses responsible for fault reactivation rather than to the ambient states of crustal stress. In this respect our conclusions are complementary to, but not directly comparable with, those of compilation studies of the current states of in situ stress (Reinecker et al., 2004).

* Corresponding author. Tel.: +44 2920 874331; fax: +44 2920 874326.
E-mail address: Lisle@cardiff.ac.uk (R.J. Lisle).

0191-8141/$ - see front matter © 2006 Elsevier Ltd. All rights reserved.
doi:10.1016/j.jsg.2006.03.012

2. Sources of data

A typical palaeostress analysis uses field data consisting of the orientations of a number of fault planes and their slip lineations measured at a single site. Incorporating the assumption that the measured faults underwent reactivation under the same overall stress conditions, the dynamic information from separate faults can be combined to constrain the possible nature of the palaeostress tensor. The results of the analysis of data from one such site are normally an estimate of an incomplete stress tensor. This so-called reduced stress tensor (Angelier, 1994) consists of the orientations of the three principal stress axes ($\sigma_1 \geqq \sigma_2 \geqq \sigma_3$, where compression is considered positive) and the ratio of the differences between the principal stress magnitudes.

Our survey of published palaeostress results includes the reduced stress tensors determined at 2791 sites. The sources of these data are listed in Appendix B. Since fault-slip analysis is only meaningful in regions where ductile strain is subordinate, the sites included are generally from areas where tectonic strain is largely accommodated by brittle deformation. The rocks involved are mainly non-metamorphic sedimentary rocks of Mesozoic and younger age, deformed at shallow crustal depths and with gentle bedding dips. According to whether the σ_1, σ_2 or σ_3 axis has the steepest plunge, the sites were classified as belonging to extensional, strike-slip or thrust/reverse settings. Of the total, 40, 39 and 21% of the sites, respectively, come from these settings. Sites are distributed geographically across all continents, though European sites dominate.

A smaller compilation consisting of 250 sets of fault-slip palaeostress results forms part of a database for the World Stress Map Project (Reinecker et al., 2004). These are not included in our database because of the risk of duplicating some of the results. The stress results that are included in our compilation were determined by a variety of stress inversion methods, all of which take account of the senses of slip on the faults and are therefore able to distinguish σ_1 and σ_3 axes (Carey and Brunier, 1974; Etchecopar et al., 1981; Angelier, 1984; Hardcastle and Hills, 1991; Sperner et al., 1993). The results derived by methods that make a priori assumptions about the stress ratio (e.g. Arthaud, 1970; Aleksandrowski, 1985) or principal stress orientations (e.g. Simón-Gómez, 1986; Fry, 1992) are not included.

3. Preferred orientation of principal stress axes

The compiled orientations of the principal stress axes are considered in relation to Anderson's hypothesis of principal stress orientations. Anderson (1951) argued that at the Earth's surface, since rock is in contact with air, the magnitude of shear stress will be of negligible magnitude. By definition, this surface must therefore be a principal plane of stress which therefore implies that one of the three principal stress directions is always close to perpendicular to the ground surface. On this basis, at shallow depths in areas with moderate topographic slope, one of the principal stresses must be near to vertical.

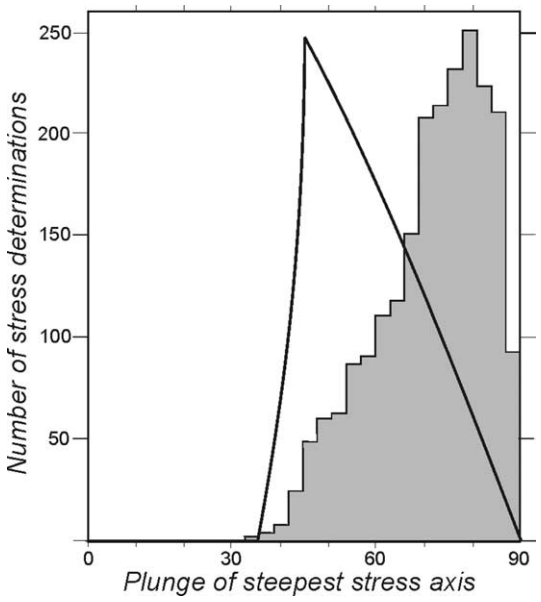

Fig. 1. Histogram showing the observed distribution of the steepest principal stress axes for 2208 palaeostress tensors. Modal plunge is 79.5°. 5, 10 and 25% percentiles are 50, 55 and 65°, respectively. The curve shows the frequency expected for random orientations of the stress axes (see Appendix A).

To test this hypothesis we examine for all sites the distribution of plunges of the steepest axis of the three principal axes (Fig. 1). Fault-slip analyses from 2208 sites reveal that one of the principal stress axes plunges at ≥ 75 and $\geq 65°$ at 46 and 75% of the total sites, respectively. The principal stress axes, σ_1, σ_2 and σ_3, are close to vertical (plunge $> 65°$) at 92, 76 and 77% of the total sites for the extensional, strike-slip and thrust/reverse fault tectonic settings, respectively (Fig. 2). The steepest axes show a modal plunge of close to 80°. However, the fact that the steepest of the three axes has been selected imparts constraints on its distribution of the plunge angles. For example, any axis plunging at greater than 45° must automatically be the steepest axis of three orthogonal axes, though a steepest axis can possess a plunge as low as 35.3°. The full significance of the observed steepest axis distribution is made clear when compared with the steepest-axis distribution expected from a three-dimensionally uniform distribution of stress axes (Fig. 1 and Appendix A). The uniform orientation model, which is characterised by a modal plunge of 45°, is significantly different from that observed.

The fact that the steepest axis has a modal plunge of approximately 80° rather than 90° appears to indicate that natural stress orientations are at odds with Anderson's one vertical axis hypothesis. However, when the observed frequencies shown in Fig. 1 are expressed as multiples of those expected from a uniform model (Fig. 3), the modal steepest axis is found to a have a vertical orientation.

When the orientations of all three stress axes are plotted stereographically (Fig. 4) the strong tendency for one axis to be vertical is seen to be matched by a preferred orientation of axes with low plunges. These low-plunging axes show no obvious

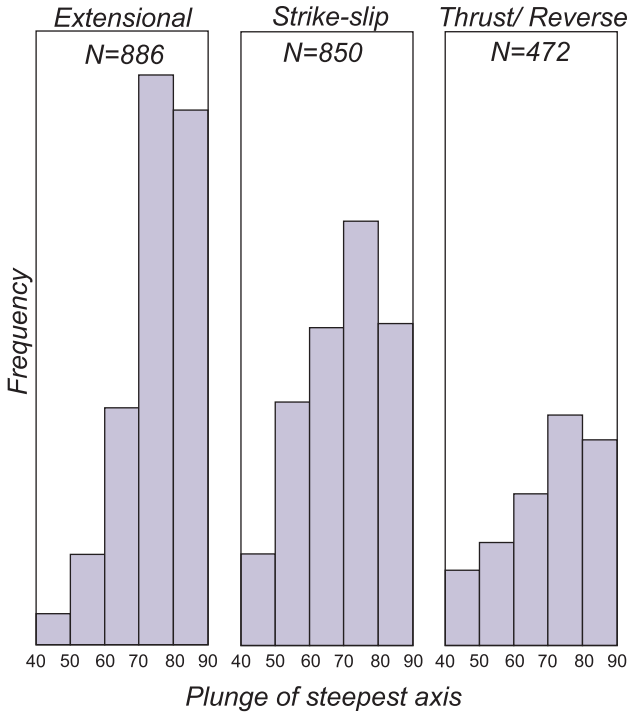

Fig. 2. Frequency of plunges for the steepest principal stress axis in cases where σ_1, σ_2 and σ_3, respectively, correspond to the steepest of the three axes.

preferred directions of plunge. This is taken to reflect the broad spread of the sample sites in terms of geography and tectonic setting.

4. Favoured shape of palaeostress ellipsoids

In addition to the orientations of the principal stresses, published results of fault-slip analyses also include a parameter that describes one aspect of the shape of the stress ellipsoid, referred to as the stress ratio. The most commonly used stress ratio is that of Bishop (1966) and Angelier (1975) defined as

$$\Phi = (\sigma_2 - \sigma_3)/(\sigma_1 - \sigma_3) \quad (1)$$

This measure is independent of the hydrostatic component of the stress tensor and describes the shape, though not the magnitude, of the deviatoric part of the tensor. This ratio ranges from zero for states of axial compressive deviatoric stress ($\sigma_1 > \sigma_2 = \sigma_3$), to one for axial tensile deviatoric stress ($\sigma_1 = \sigma_2 > \sigma_3$). When Φ equals 0.5, σ_2 is the arithmetic mean of σ_1 and σ_3, and corresponds to plane deviatoric stress. Some publications have used other definitions of the stress ratio, which were converted to Φ values using the equations of Orife and Lisle (2003), e.g.

$$R = (\sigma_2 - \sigma_3)/(\sigma_1 - \sigma_2) = \Phi/(1 - \Phi) \quad (2)$$

(Lisle, 1979)

$$R = (\sigma_1 - \sigma_2)/(\sigma_1 - \sigma_3) = 1 - \Phi \quad (3)$$

(Carey and Mercier, 1987) and

$$\mu = [(\sigma_1 - \sigma_2) - (\sigma_2 - \sigma_3)]/(\sigma_1 - \sigma_3) = 1 - 2\Phi \quad (4)$$

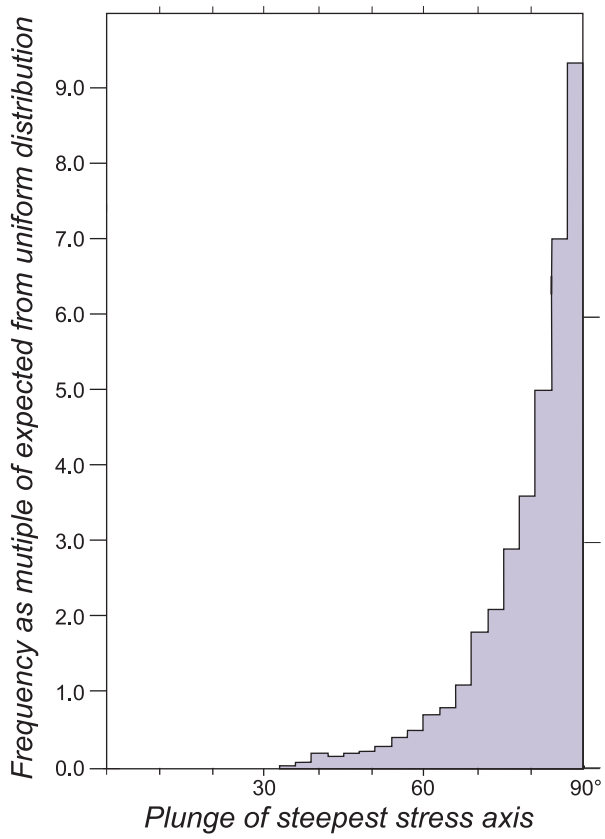

Fig. 3. Observed frequencies of plunge angles of steepest axis expressed as multiples of those expected from a uniform orientation distribution of stress axes (thick line in Fig. 1).

(Nádai, 1950, p. 107)and, with the help the equations in Orife and Lisle (2003), the stress ratios compiled from 2791 sites (see source list in Appendix B) were converted to a common stress ratio, Φ. The obtained frequencies of stress ratios are found to be non-uniformly distributed (Fig. 5). Two observations can be made about this distribution: First, the histogram reveals that Φ values in the middle range are much more abundant than the extreme values around 0 and 1. This indicates a preference in the Earth's crust for plane deviatoric stress states relative to axial compression or axial tension stress states. Given the large sample size, there can be no doubt about the statistical significance of this observation. Second, there is an asymmetry in the distribution with respect to $\Phi = 0.5$. Namely, values of Φ ranging between 0 and 0.5 appear about 2.3 times more often ($n = 1550$) than Φ values ranging from 0.5 to 1.0 ($n = 658$) (Fig. 5). The mean value of Φ for all our compiled results is 0.39. Results of a similar type, obtained from the World Stress Map Project database, have a mean Φ value of 0.38. A further test of the inference regarding the bias towards the axially compressive state of stress was made by classifying the data into normal, strike slip and reverse/thrust fault types of tectonic settings. This classification was achieved by distinguishing three separate groups of tensors on the basis of whether σ_1, σ_2 or σ_3 axes plunge at very steep angles $\geq 75°$, respectively. For all three groups there is a relative lack in Φ values greater than 0.5 (Fig. 6) but their distributions, according to the

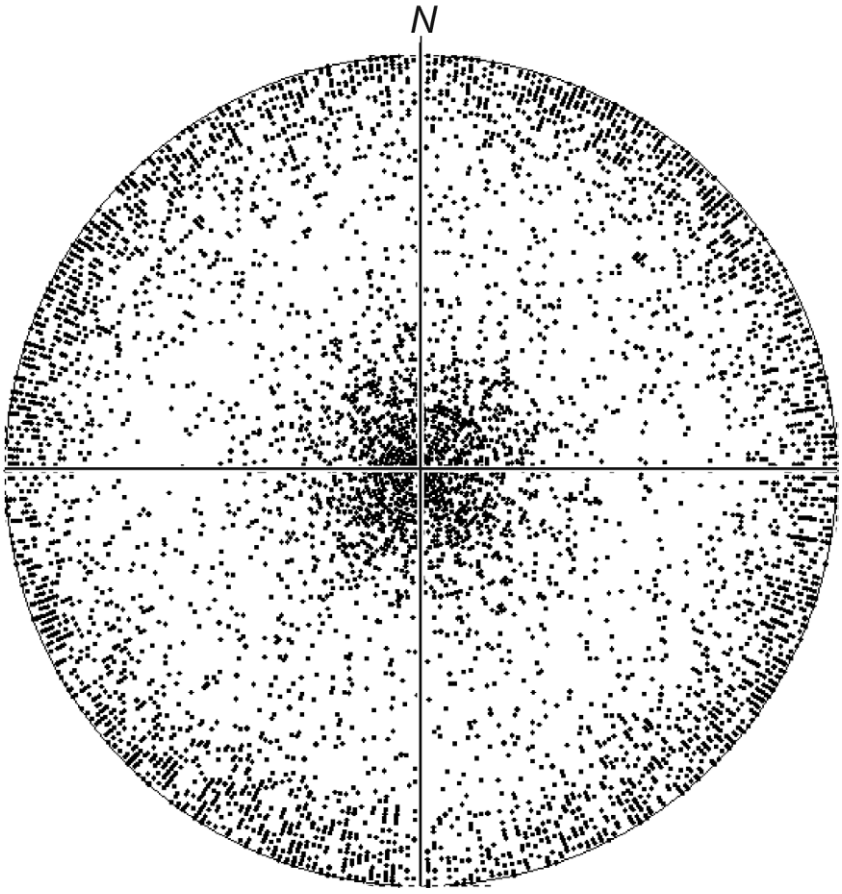

Fig. 4. Stress orientations, σ_1, σ_2 and σ_3, for all compiled analyses (lower hemisphere, equal-area stereogram).

Kolmogorov–Smirnov test (see Cheeney (1983, p. 45) for details), are significantly different. In particular, the 'normal-fault' stress states have the lowest mean Φ of 0.34, whilst thrust/reverse states give the highest mean of 0.43.

Before seeking a geological explanation for this non-uniform distribution of stress ratios it seems logical to question whether the observed bias may be a statistical artefact. A simple random number experiment was used to check this. Three random numbers were chosen within the range 0–1. According to their relative magnitudes, the principal stresses were assigned these values. After repeated trials, the Φ values of such random stresses are found to exhibit a uniform frequency distribution. Other studies, however, suggest that this process does not produce tensors with a uniform distribution. For example, Orife (2001) determined reduced stress tensors from artificial datasets consisting of collections of randomly chosen fault planes possessing random slip lineations. The Φ values of these tensors do not display a uniform frequency distribution; the histogram is bell-shaped with a mode at $\Phi = 0.5$. Sato and Yamaji (2006) construct a population of 60,000 reduced stress tensors, which are arranged on a four-dimensional grid, and where the stress difference (Orife and Lisle, 2003) between neighbours is close to uniform. This uniform distribution of tensors is also characterized by a bell-shaped distribution of their Φ values.

Would another parameter lead to a more uniform frequency distribution? In this regard, it can be shown that all the commonly used stress ratios are linear functions of Φ (Orife and Lisle, 2003); therefore the frequency distributions of these parameters will be similar to that of Φ.

It could be argued that a more 'natural' shape parameter for fault-slip results would be one that relates directly to the angular variation of the striae (the assumed shear stress direction) in the fault plane. Since the theoretical shear stress direction depends on the orientation of the plane as well as on the stress shape parameter, we consider the shear stress direction on a special 'octahedral' fault plane; one that is inclined equally with respect to all three stress axes (Fig. 7a). Using a simplification of Bott's (1959) equation, the pitch of the shear stress direction in the plane of the fault, θ, measured with respect to the line of intersection of the $\sigma_1\sigma_3$ plane, is found to equal:

$$\theta = \tan^{-1}[(1-2\Phi)/\sqrt{3}] \tag{5}$$

This equation demonstrates that the orientation of slip direction on the octahedral fault plane is a function only of the shape ratio of the stress tensor. It follows from this that the angle θ could be used as an alternative to Φ as an index of the stress ellipsoid's shape. However, since θ is a non-linear function of Φ, their frequency distributions will differ. Fig. 7b

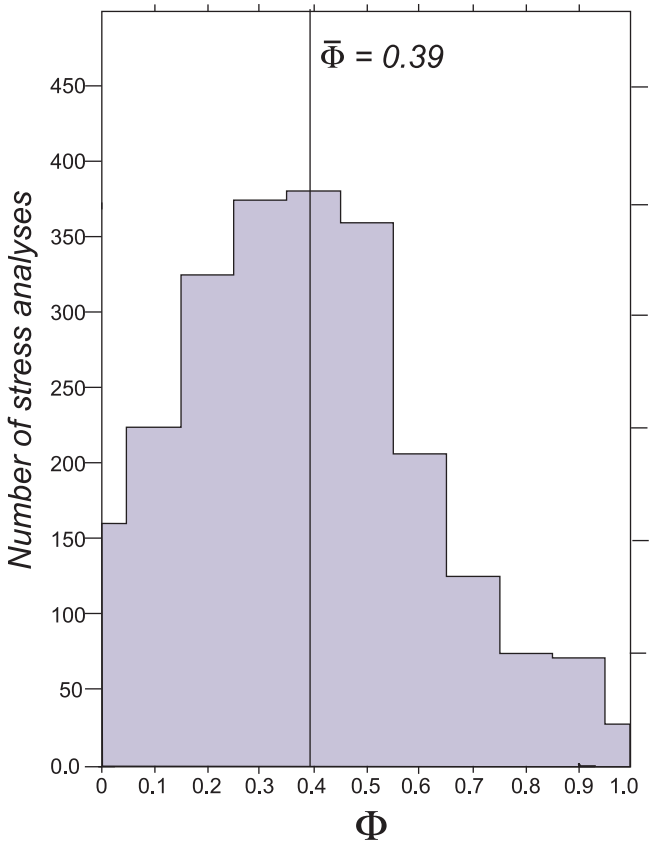

Fig. 5. Observed distribution of stress ratios, Φ, compiled from all fault-slip analyses.

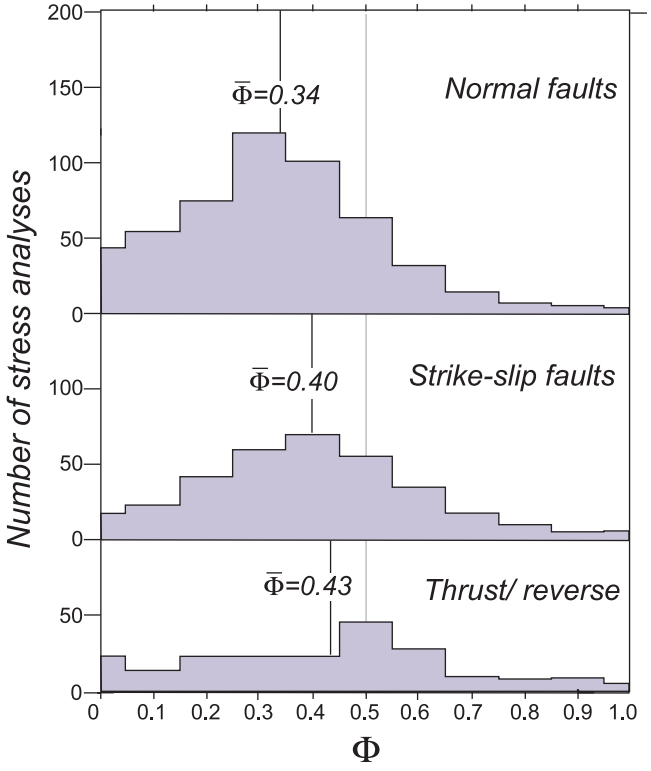

Fig. 6. Distribution of Φ values for different stress regimes (normal, strike-slip and thrust faults) with σ_1, σ_2 and σ_3, respectively, at plunging at angles ≧75°. For normal, strike-slip and thrust fault regimes, Φ values less than 0.5 account for 82, 72 and 61% of the total number of values, respectively.

is the circular histogram of all stress ratios collated in our survey, plotted as θ values instead of Φ. On this new graph stress states corresponding to axial compression deviatoric stress ($\Phi=0$) and axial tension deviatoric ($\Phi=1$) plot along lines of θ equal to 30 and $-30°$, respectively, whilst plane deviatoric stress ($\Phi=0.5$) plots along the $\theta=0°$ line. However on the new form of display the paucity of axial stress states and skewness of the histogram of θ values remains evident (Fig. 7b) and is as pronounced as in the corresponding histogram for Φ (Fig. 5).

The disadvantage of the θ parameter is, like Φ, that a random sample from a uniform distribution of tensors does not lead to a uniform distribution of the shape parameter. In the absence of the correct parameter in this respect, we have corrected the frequencies of Φ values in Fig. 5 to allow for the fact that a uniform distribution of stresses leads to a predominance of Φ in the middle range. The resulting histogram (Fig. 8) expresses the frequencies of different Φ values as multiples of those expected from a uniform distribution of tensors (Sato and Yamaji, 2006). This corrected histogram is very different from the uncorrected distribution (Fig. 5). It demonstrates that natural stress ratios, when compared with those expected from a uniform distribution of stress states, show a preference for axial stress states at the expense of triaxial stresses. However, the corrected histogram confirms the observed preference for low Φ values in natural stress ratios. The corrected mean Φ value is 0.29, with values less that 0.5 being three times more abundant than those above 0.5.

We now seek possible geological explanations for the observed unequal abundances of different Φ ratios.

5. Possible explanations for favoured shape of stress ellipsoid

5.1. Plane strain condition

The observation that palaeostress ratios are skewed towards lower stress ratio values (Figs. 5, 6 and 8) may be explained by considering the constraints on strain patterns in the Earth's crust. Although complex in detail, there is often a tendency for tectonic structures to occur in linear trends with continuity of individual structures in clearly defined trends and with maintenance of transverse cross-sectional structural geometry on planes perpendicular to the longitudinal direction. Furthermore, the intraplate stress trajectories are often uniform in direction over large parts of continents (Zoback et al., 1989; Zoback, 1992). This tendency for linear structural continuity will restrict the ability of crustal rocks to suffer elongation or shortening in the direction of the structural trend, a condition producing a tendency towards plane strain.

This plane strain condition leads to special relationships between the principal stresses. Let us assume that σ_V, σ_T and σ_L are principal stresses, respectively, parallel to the vertical,

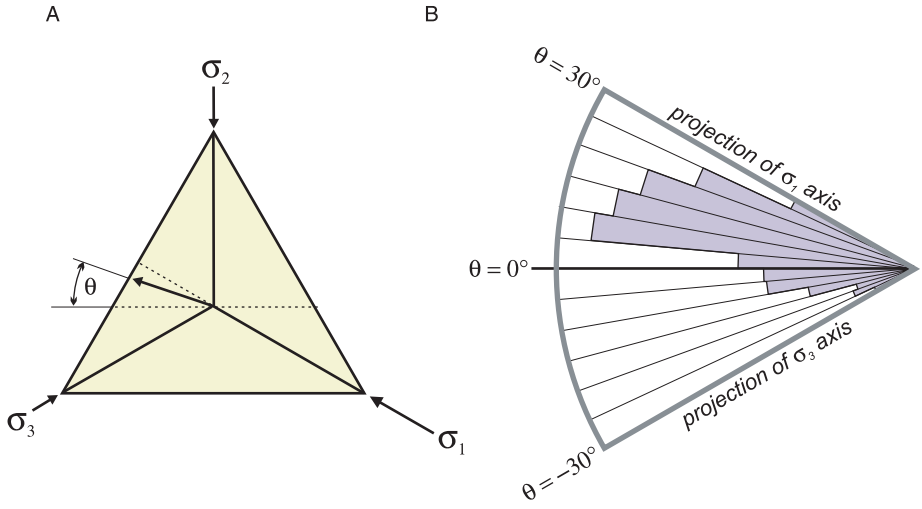

Fig. 7. Alternative shape index for stress tensors. (A) Orientation of the theoretical shear stress direction on the octahedral plane recorded by the angle θ, an alternative index of shape. (B) Circular histogram of θ values reveals a strong preference for positive values (i.e. Φ values less than 0.5).

transversal and longitudinal directions in a deformation belt, whilst e_V, e_T and e_L are the corresponding strains in those directions. Elastic strains and stresses in isotropic rocks are related by equations given, for example, by Ramsay and Lisle (2000, p. 721). Specifically, the strain in the longitudinal direction e_L is given by:

$$e_L = -\frac{1}{E}\left[\sigma_L - \nu(\sigma_T + \sigma_V)\right] \quad (6)$$

where E and ν are elastic constants, Young's modulus and Poisson's ratio, respectively.

If plane strain applies (i.e. $e_L = 0$) it follows that

$$\sigma_L = \nu(\sigma_T + \sigma_V) \quad (7)$$

If deformation occurs at constant volume, i.e. the rocks involved are incompressible, the value of the elastic constant ν equals 0.5. Therefore, according to Eq. (7), this would always lead to one principal stress being the mean of the other two stresses, i.e. plane deviatoric stress ($\Phi = 0.5$). This plane strain effect would produce the relative abundance of intermediate stress ratios compared with those close to zero or one and would not explain the bias towards values of Φ less than 0.5.

An additional consideration is that rocks are in reality compressible to various degrees; the Poisson's ratios compiled for igneous, metamorphic and sedimentary rocks by Carmichael (1982) has an average close to 0.16. Fig. 9 shows the possible combinations of principal stresses compatible with the plane strain assumption and a value of Poisson's ratio, ν, of 0.16. The relative magnitudes of σ_V, σ_T and σ_L calculated from Eq. (7) correspond to the contrasting faulting configurations of thrusts, strike-slip and normal faults aligned in longitudinal or transverse directions as shown in Fig. 9. If both vertical and transverse stress components are positive (σ_V, $\sigma_T > 0$), the expected stress orientations correspond to longitudinal thrusts (i.e. thrust faults that strike along the orogenic belt), transverse strike-slip faults and normal faults with both longitudinal and transverse orientations.

The plane strain assumption with $\nu = 0.16$, also leads to a complete range of stress ratio values as shown in Fig. 10. Even if the restriction of positive transverse and vertical stress components is applied, potential Φ values are found to vary from 0 to 1. However, not all of the stress configurations on Fig. 10 are likely to be recorded by fault-slip analysis because only certain stress states are likely to lead to fault reactivation.

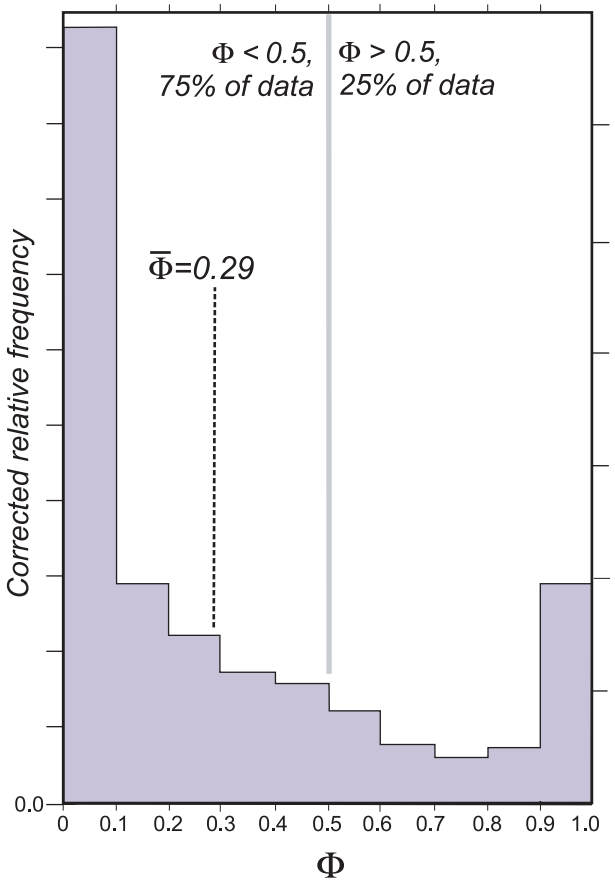

Fig. 8. Corrected distribution of Φ values, showing the frequencies as multiples of those expected from a sample from uniform population of stress tensors.

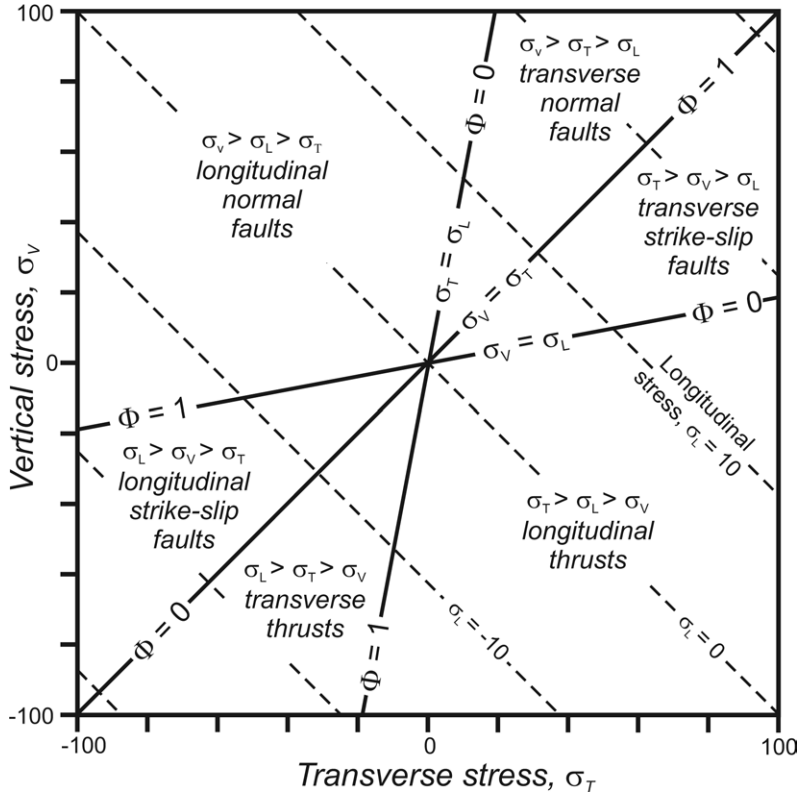

Fig. 9. Permissible combinations of principal stresses under conditions of plane strain ($e_L = 0$) and a Poisson's ratio of 0.16. Orientations of the principal stress axes vary with position on this plot. Stress values apply for all choices of stress units.

We use a frictional theory of reactivation to constrain the stresses that lead to fault slip. Using a straight sliding envelope and the assumption of zero cohesion, the principal stresses sufficient to overcome friction fulfil the condition that

$$\sin\phi = \frac{\sigma_1 - \sigma_3}{\sigma_1 + \sigma_3}$$

where ϕ is the angle of sliding friction. Using typical angles of friction of between 20 and 40° (Byerlee, 1978), these stresses for reactivation are given graphically by Fig. 10. These stresses give rise to Φ values below 0.5, in the range 0.0–0.3. If a higher value of ν is chosen, the resulting Φ value increases towards 0.5. This explanation involving plane strain with volume reduction is therefore capable of producing Φ values typical of those observed in nature.

5.2. Contribution of overburden stresses

Another possible explanation of the observed variation of stress ratio values for crustal stress states involves consideration of the ubiquitous contribution made by the rock overburden to the total state of stress. The nature of the stress tensor at depth arising from the load of overlying strata will depend on rock elastic constants and on any anisotropy of these constants. In the present discussion we assume the rock overburden stresses to have a vertically oriented σ_1 and with σ_2 and σ_3 equal in magnitude. They are thus stress states with Φ = 0 and a differential stress value that can vary, e.g. as a function of depth or mechanical properties. The present model ignores the possible effects of strain constraints discussed in the previous section. We then consider the total stress that would arise from the superimposition of such overburden stresses upon stresses of tectonic origin. Since the latter are difficult to constrain for the general case we are obliged to consider a complete range, whilst assuming one stress axis to be vertical.

The calculation of the stresses produced by the superimposition of two stress states is straightforward because the stress components are coaxially aligned (Ramsay, 1967, p. 44) and can be graphically illustrated by means of Nádai's (1950) stress diagram (Fig. 11). Stress states are described in terms of the principal stress magnitudes; of the vertical principal stress σ_V and of the two horizontal axes aligned in two arbitrary directions σ_H and σ_h. The Nádai diagram is a 2D projection of a three-axis Cartesian graph, in which stress states are represented by points σ_v, σ_H and σ_h. By viewing the 3D graph along a direction inclined equally with respect to the three axes, i.e. along the direction $\sigma_V = \sigma_H = \sigma_h$, information about the hydrostatic stress component of the stress tensor is sacrificed but with the desirable result that projected points on the Nádai diagram describe only the three principal deviatoric stresses of the stress state. Stress states plot at a distance from the origin that conveys the overall level of deviatoric stress. This form of display is well suited to the modelling of stresses in terms of their Φ values, because Φ describes a characteristic of the deviatoric stress tensor and is independent of the hydrostatic stress. Contours of constant Φ form radial lines and the general orientations of the principal stress axes are portrayed in relation to sectors of the graph corresponding to

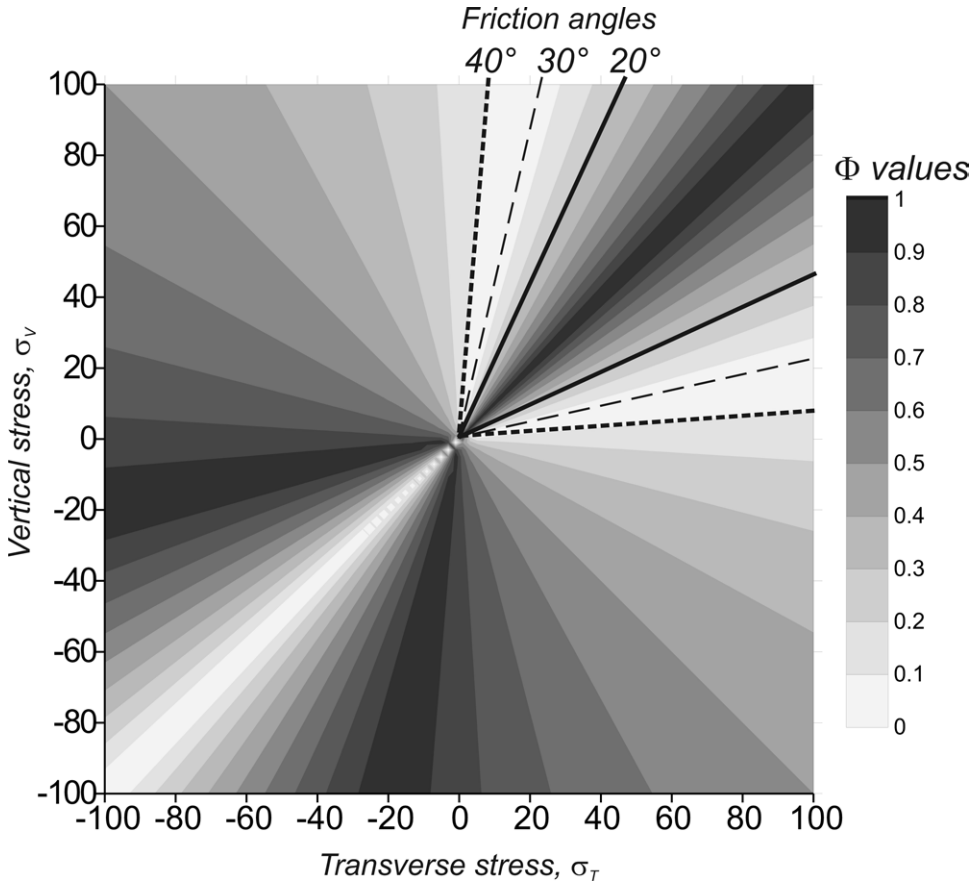

Fig. 10. Under assumptions of plane strain and a Poisson's ratio of 0.16, compressive stress states consistent with fault reactivation lie on straight lines and depend on the angle of sliding friction. The stress ratios of stress states compatible with plane strain are shown as shading. For friction angles in the range 20–40°, the reactivating stresses have stress ratios varying from 0.3 to 0.1.

normal, strike-slip and thrust stress orientations (Fig. 11). A practical benefit of the Nádai diagram is that it displays the results of stress superimposition in a simple and direct manner. The superimposition of two stress states is performed on the plot as a vector addition (Fig. 10b).

We use the Nádai diagram to consider the Φ values of the stress tensors resulting from the superimposition of tectonic and overburden stresses. The latter are stresses with $\sigma_v > \sigma_H = \sigma_h$ and are represented by points like L in Fig. 11c. Many tectonic stresses, with all possible orientations and Φ values but with constant magnitude, plot as points lying on a circle centred on the origin (Fig. 11c). The resulting combined stresses are given by the assemblage of points on the circle translated by the overburden stress vector. Depending on the relative magnitude of overburden, the stress points migrate out of the thrust field, through the strike-slip fault field and into the field of normal fault orientations. A prediction of this model is therefore that stresses with 'normal' orientation would dominate, whilst the number of thrust orientations would become depleted as the overburden stress increases. This agrees with their observed relative abundances in our compiled data. Fig. 12 shows the results for different levels of overburden stress relative to the tectonic stress. For overburden stresses that are low in magnitude compared with the tectonic stress, the average Φ of the combined stresses is close to 0.5. The average Φ rises to 0.6 as the relative level of the overburden stress increases to 1.1, but thereafter falls with increasing overburden. If the overburden stress reaches a level double the tectonic component the average Φ falls to 0.32. To obtain the observed average Φ of 0.29 would require a value of overburden stress equal to 2.3 times greater than the tectonic stress component.

In this simulation of the effects of stress superimposition the distribution of Φ changes with magnitude of overburden (Fig. 12). As the overburden component increases there is a loss of symmetry so that the distributions become positively skewed.

5.3. Other factors affecting stress ratios

Since the majority of the stress analyses come from regions where the bedding show gentle dips ($<20°$) it is likely that the relative magnitudes of horizontal and vertical stresses are influenced by anisotropy of elastic properties. In addition, the presence of preferred orientation of faults prior to their reactivation will impart mechanical anisotropies on the rock mass. However, no attempt has been made here to anticipate the possible effects on the average stress ratios.

Another issue not considered in detail is the effect of the magnitude of the intermediate principal stress on the strength

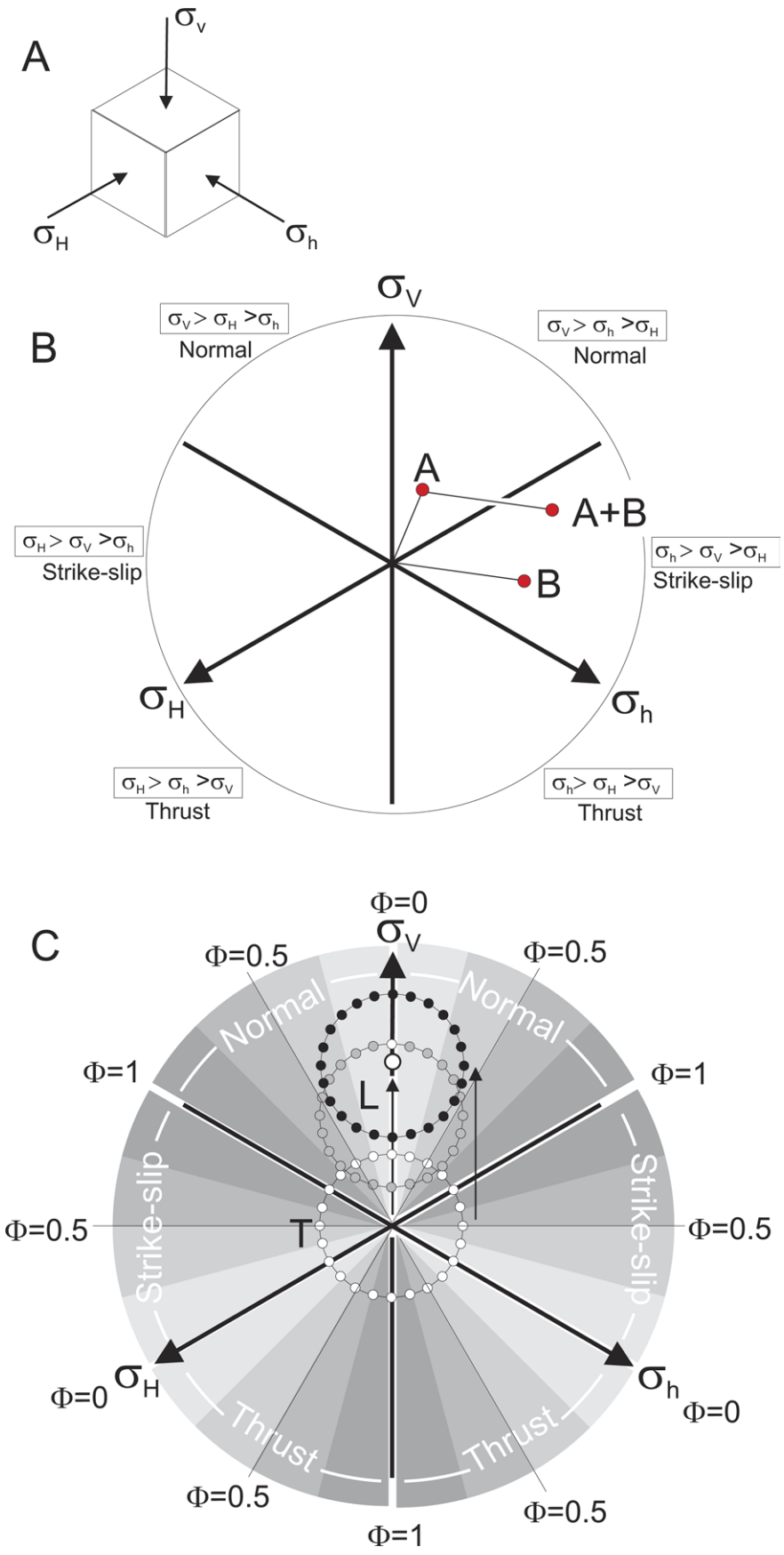
A
σV
σH
σh
B
σV> σH >σh
Normal
σV> σh >σH
Normal
A
A+B
B
σH> σV >σh
Strike-slip
σh> σV >σH
Strike-slip
σH
σh
σH> σh >σV
Thrust
σh> σH >σV
Thrust
C
Φ=0
σV
Φ=0.5
Φ=0.5
Normal
Normal
Φ=1
Φ=1
L
Strike-slip
Strike-slip
Φ=0.5
T
Φ=0.5
Φ=0
σH
σh
Φ=0
Thrust
Thrust
Φ=0.5
Φ=0.5
Φ=1

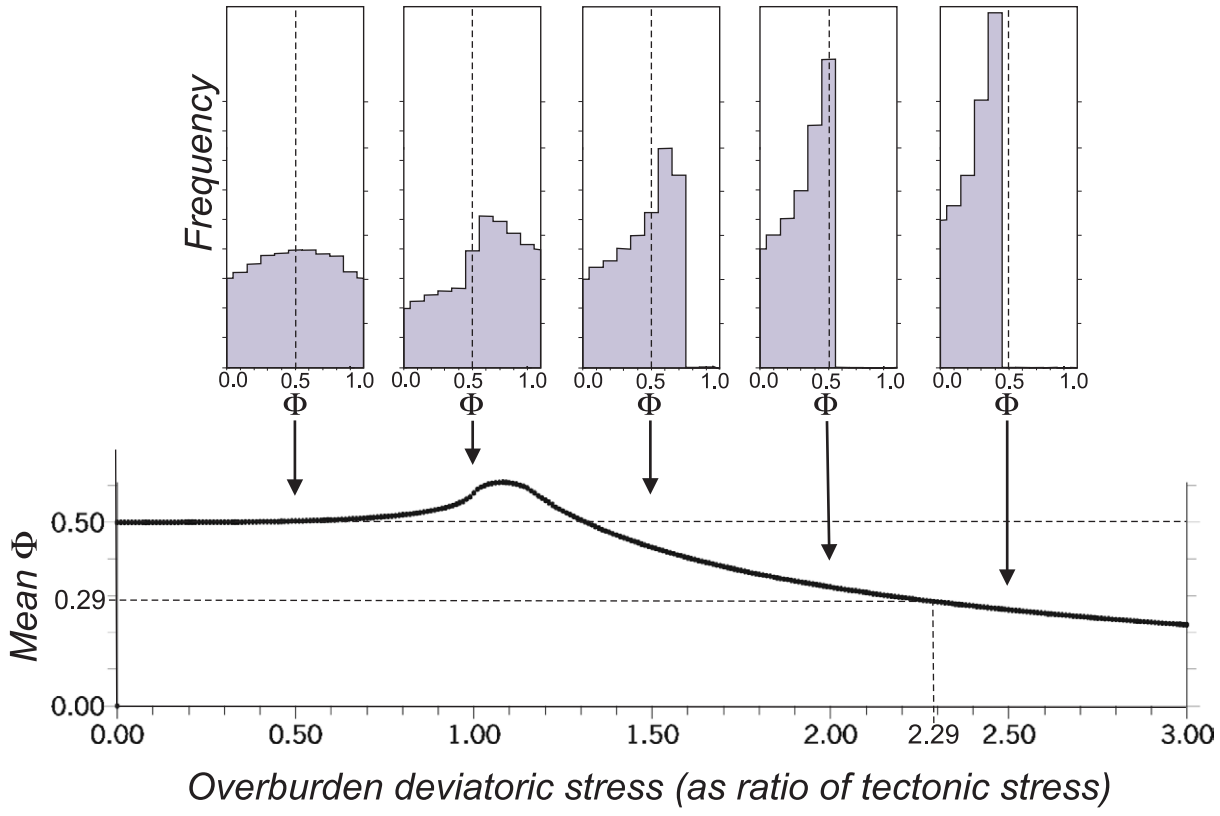

Fig. 12. Average stress ratio (Φ) and the distribution of Φ values obtained from the stress modelling explained in Fig. 11, where an axial overburden stress is superimposed on tectonic stresses of constant magnitude, but with a complete range of Φ and axial orientations. The average Φ value of 0.29, observed in natural palaeostress results, is produced by an overburden stress that is 2.29 times greater (in terms of the octahedral shear stress) than the tectonic stress component.

of the rock mass. At least in relation to newly formed fractures, some authors have suggested (reviewed by Paterson, 1978, p. 39) that the shear strength may increase with σ_2. Also, in relation to reactivation of existing faults, the increase in average normal stress concomitant with higher σ_2 may have the effect of inhibiting reactivation when the Φ value is high and thus possibly leading to a relative dominance of reactivation under low Φ stress states.

6. Discussion and conclusions

The results of palaeostress analysis are not necessarily a reflection of typical stress states in the crust; they are a record of stress states at abnormal times of fault reactivation. For this reason the dominant stress configurations observed in this survey may not be comparable with average 'snapshot' stress conditions in the upper crust.

The preferred orientation patterns of the axes of the compiled stress tensors are quite unlike those expected from random sampling of a uniform orientation distribution. In particular, there is a strong tendency for one of the stress axes to have a near-vertical orientation. Our analysis of results is in general support of the 'one vertical axis' theory of Anderson (1951). On the other hand, in 25% of the sampled tensors the steepest axis deviated by more than 25° from the vertical. This could be due to the fact that Anderson's assertion would not apply to deeper depths away from the Earth's free surface. In addition, deviation from verticality could be due to non-horizontal topography, to body rotation, or folding may have affected some sites after reactivation, to mechanical inhomogeneities, or to complex deflection of stress trajectories in the vicinity of large-scale faults or other relatively weak horizons. Whatever the causes, our study indicates that it would be unwise to apply methods of stress inversion that assume that one stress axis is always vertical, though this may be justified in particular local regions.

Stress orientations corresponding to normal and strike-slip faulting are most common within the assembled palaeostress

Fig. 11. Use of the Nádai diagram to illustrate the modelling of stress superimposition. (A) The principal stress axes are assumed to be parallel to three reference directions; one vertical (σ_v) and the other two horizontal (σ_h, σ_H). (B) Nádai stress diagram with plotted stress states A and B. Diagram represents the 2D projection of the stress state onto the octahedral plane. Distances of plotted points from the origin are proportional to the magnitude of the deviatoric stresses expressed by the octahedral shear stress (see Orife and Lisle, 2003). Superimposition of these stresses is performed by vector addition. (C) Nádai diagram, shaded according to Φ values. Tectonic stresses with complete range of orientations and shape ratios define a circle T (white). The stress states have equally distributed Φ values. When a vertical overburden stress is imposed, the combined stresses form a circular pattern displaced upwards (grey). Stress states with $\Phi > 0.5$ are more frequent than $\Phi <$

results (40 and 39%, respectively.), followed by thrust configurations with only half the frequency (21%). It cannot be discounted that this observation is in part due to the fact that the sites of the compiled analyses are located preferentially in certain different tectonic settings.

In terms of stress ratios, there is a general lack of stress states of high Φ type, with 75% of Φ values lying between 0 and 0.5. This confirms the suggestion of Lisle (1979) who, in the infancy of palaeostress analysis, noted a preference for low Φ values. There are several possible explanations for these patterns, including the modification of tectonic stresses by superimposition of $\Phi=0$ stress components due to overburden loading. This idea accounts for the relative dominance of stress orientations corresponding to normal faults, but does not explain well the shape of the frequency histograms of natural Φ values. However, the importance of the simulated histograms should not be overemphasised, since they depend strongly on the assumed nature of the tectonic stress tensors.

An alternative explanation put forward to explain the observed distribution of Φ values involves the assumption that crustal strains show some tendency towards plane strain. This leads to stresses with $\Phi=0.5$ or lower, depending on the value assumed for Poisson's ratio. According to this, the abundance of Φ values less than 0.5 is ascribed to volume reduction during deformation. In this respect this explanation is similar to that used by Ramsay and Wood (1973) to explain the prevalence of prolate shapes of finite strain ellipsoids.

In summary we have demonstrated that palaeostress tensors exhibit well defined patterns, both in terms of principal stress orientations and in terms of stress ratios. Regarding the latter, we are unable to ascribe the observed pattern to one particular effect, though we have been able to identify a number of possible contributing factors.

Acknowledgements

We thank Tom Blenkinsop and Norman Fry for discussions. The paper benefited from thorough reviews by Blanka Sperner and John Townend.

Appendix A. Distribution of plunges of the steepest stress axes for random stress states

For the σ_1 axis, the probability of a given plunge angle (x_1), expressed as a multiple of that expected from a uniform distribution, is:

$$P_1 = \cos(x_1)$$

For a given x_1, the plunge of σ_2, (x_2), is given by:

$$\sin(x_2) = \sin\rho_2 \sin(90 - x_1) = \sin\rho_2 \cos(x_1)$$

where ρ_2 is the pitch of σ_2 in the $\sigma_2\sigma_3$ plane.

The stress axes σ_2 and σ_3 have random pitches in the $\sigma_2\sigma_3$ plane. The pitch of σ_2 ($=\rho_2$) corresponding to the situation that x_1 equals x_2 is given by:

$$\sin\rho_2 = \sin x_1/\cos x_1 = \tan x_1$$

i.e. ρ_2 (when x_1 equals x_2) $=\sin^{-1}(\tan x_1)$.

It can be shown that the probability that $x_1 > x_2$ and $x_1 > x_3 = (\rho_2 - 45)/90$.

There is no solution when $x_1 > 45°$. This implies that there is no line in the $\sigma_2\sigma_3$ plane with a plunge steep enough to exceed the plunge of σ_1. Therefore if the plunge of any axis is greater than 45° that axis must be the steepest one.

A.1. What is the minimum plunge of a steepest axis?

When x_1 equals x_2,

$$\rho_2 = \sin^{-1}(\tan x_1)$$

By setting ρ_2 equal to 45° in this equation, we discover the least possible plunge for a steepest axis. This is $\tan^{-1}(\sin 45) = 35.26°$.

The probability that a plunge of x_1 is the steepest axis is therefore found to be proportional to:

$$\cos x_1, \quad \text{when} \quad x_1 > 45°,$$

$$\cos x_1 \{\sin^{-1}[\tan x_1] - 1\}/45, \quad \text{when} \quad 45° > x_1 > 35.26°$$

and

$$0, \quad \text{when} \quad x_1 < 35.26°.$$

This theoretical distribution of the steepest axis is shown in Fig. 1. Maximum frequency occurs for a plunge of 45°, a feature very different to the distribution of the steepest axes from compiled stresses. Therefore the latter are clearly not random but possess a significant preferred orientation in a vertical orientation. The modal plunge is approximately 80°.

Appendix B. Source list

Ait Brahim, L., Chotin, P., Hinaj, S., Abdelouafi, A., El Adraoui, A., Nakcha, C., Dhont, D., Charroud, M., Sossey Alaoui, F., Amrhar, M., Bouaza, A., Tabyaoui. H., Chaouni, A., 2002. Paleostress evolution in the Moroccan African margin from Triassic to Present. Tectonophysics 357, 187–205.

Aldrich, M.J. Jr, Adams, A.I., Escobar, C., 1991. Structural geology and stress history of the Platanares geothermal site, Honduras; implications on the tectonics of the northwestern Caribbean Plate boundary. In: Goff, F. (Ed.), Honduras; a Geothermal Investigation. Journal of Volcanology and Geothermal Research 45, pp. 59–69.

Anderson, R.E., Barnhard, T.P., 1986. Genetic relationship between faults and folds and determination of Laramide and neotectonic palaeostress, western Colorado Plateau-transition Zone, central Utah. Tectonics 5, 335–357.

Angelier, J., 1984. Tectonic analysis of fault-slip data. Journal of Geophysical Research 89, 5835–5848.

Angelier, J., 1989. From orientation to magnitudes in paleostress determinations using fault slip data. Journal of Structural Geology 11, 37–50.
Angelier, J., 1990. Inversion of field data in fault tectonics to obtain the regional stress. III. Geophysical Journal International 103, 363–376.
Angelier, J., 1994. Failles, non-failles et structures de pression/tension dans l'inversion des données de tectonique cassante en termes de tenseurs des contraintes. Bulletin de la Société Géologique de France 165, 211–219.
Audemard, M.F.A., 2001. Quaternary tectonics and present stress tensor of the inverted northern Falcon Basin, northwestern Venezuela. In: Dunne, W.M., Stewart, I.S., Turner, J.P. (Eds.), Paul Hancock Memorial Issue. Journal of Structural Geology 23, pp. 431–453.
Averbuch, O., Lamotte Frizon de, D., Kissel, C., 1993. Strain distribution above a lateral culmination: an analysis using microfaults and magnetic fabric measurements in the Corbieres thrust belt (NE Pyrenees, France). Annales Tectonicæ 7, 3–21.
Barrier, E., Angelier, J., 1983. Étude d'une compression subactualle dans un contexte de collison: la déformation des conglomerats de Pinanshan (Taïwan, République de Chine). Bulletin de la Société Géologique de France 25, 229–238.
Barrier, E., Angelier, J., Chu, H.T., Teng, L.S., 1982. Tectonic analysis of compressional structure in an active collision zone: the deformation of the Pinnanshan conglomerates, eastern Taiwan. Proceedings of the Geological Society China 25, 123–138.
Bellier, O., Zoback, M.L., 1995. Recent state of stress change in the Walker Lane zone, western Basin and Range Province, United States. Tectonics 14, 564–593.
Bergerat, F., 1981. États de contrainte tertiaires liés á la tectonique cassante dans le sud de la vallée due Rhóne. Dynamique des failles gardoises de direction varisque. Comptes Rendus de l'Academie des Sciences Paris 293, 925–928.
Bergerat, F., 1987. Stress fields in the European Platform at the time of Africa–Eurasia collision. Tectonics 6, 99–132.
Bergerat, F., Geyssant, J., 1982. Tectonique cassante et champ de constraintes tertiaire en avant des Alpes orientales; le Jura souabe. Geologische Rundschau 71, 537–548.
Bergerat, F., Martin, P., 1994. Analyse de failles du forage Balazuc-1 (programme GPF) et reconstitution des paléo-états de contrainte sur la bordue vivaro-cévenole do bassin du Sud-Est de la France. Relations avec la marge européene de la Téthys ligure. Bulletin de la Société Géologique de France 165, 307–315.
Bergerat, F., Pironkov, P., 1994. Deformations cassantes et contraintes crétacées à actuelles dans la plate-forme moesienne (Bulgarie). Bulletin de la Société Géologique de France 165, 447–458.
Bergerat, F., Vandycke, S., 1994. Palaeostress analysis and geodynamical implications of Cretaceous–Tertiary faulting in Kent and the Boulonnais. Journal of the Geological Society of London 151, 439–448.
Bergerat, F., Bergues, J., Geyssant, J., 1985. Estimate of palaeostress connected to the formation of transverse faults in the Northern European Platform. Geologische Rundschau 74, 311–320.
Bernini, M., Coccaletti, M., Gelati, R., Moratti, G., Papani, G., Tortorici, L., 1990. The role of E–W transpressive movements in the evolution of the Neogene basins of the Betic Cordillera. Annales Tectonicæ 4, 81–95.
Berry, R.F., 1989. The history of movement on the Henty fault zone, western Tasmania: an analysis of fault striations. Australian Journal of Earth Sciences 36, 189–205.
Boccaletti, M., Getaneh, A., Tortorici, L., 1992. The main Ethiopian rift; an example of oblique rifting. Annales Tectonicæ 6, 20–25.
Boncio, P., Brozzetti, F., Lavecchia, G., 1996. State of stress in the Northern Umbria–Marche Appenines (central Italy). Annales Tectonicæ 10, 80–97.
Brozzetti, F.N., Lavecchia, G., 1994. Seismicity and related extensional stress field: the case of Norcia seismic zone. Annales Tectonicæ 8, 36–57.
Brozzetti, F.N., Lavecchia, G., 1995. Evoluzione nel campo degli sforzi e storia deformativa nell'area dei Monti Martani (Umbria). Bollettino della Societa Geologica Italiana 114, 55–176.
Burg, J.P., Etchecopar, A., 1980. Détermination des systémes de constraintes liés à la tectonique cassante au coeur du Massif Central Francais; la région de Brioude (Haut-Allier). Comptes Rendus de l'Academie des Sciences Paris, 290, 397–400.
Burg, J.P., Teyssier. C., Lespinasse. M., Etchecopar, A., 1982. Direction de contraintes et dynamique du bassin de Saint Flour–Saint Alban (Massif Central francais) a l'Oligocene. Comptes Rendus de l'Academie des Sciences Paris 294, 1021–1024.
Cabrera, J., Sebrier, M., Mercier, J.L., 1987. Active normal faulting in high plateaus of central Andes: the Cuzco region (Peru). Annales Tectonicæ 1, 116–138.
Carey-Gailhardis, E., Mercier, J.L., 1987. A numerical method for determining the state of stress using focal mechanisms of earthquake populations; application to Tibetan telseisms and microseismicity of southern Peru. Earth and Planetary Science Letters 82, 165–179.
Carrier, A., Michel, J., Angelier, J., Holyland, P., 2000. The Silidor Deposit, Rouyn-Noranda District, Abitibi Belt: geology, structural evolution, and palaeostress modelling of an Au quartz vein-type deposit in an Archaen trondhjemite. Economic Geology 95, 1049–1065.
Casas-Sainz, A.M., Gil-Pena, I., Simón-Gómez, J.L., 1990. Los métodos de análisis de paleoesfuerzos a partir de poblaciones de fallas; sistemática y técnicas de aplicación. Estudios Geológicos (Madrid) 46, 385–398.
Delvaux, D., Levi, K., Kajara, R., Sarota, J., 1992. Cenozoic paleostress and kinematic evolution of the Rukwa, North Malawi rift valley (East African system). Bulletin des Centres de Recherches Exploration-Production Elf-Aquitaine 16, 383–406.

Delvaux, D., Kervyn, F., Vittori, E., Kajara, R.S.A., Kilembe, E., 1998. Late Quaternary tectonic activity and lake level change in the Rukwa Rift Basin. Journal of African Earth Sciences 26, 397–421.

Doutsos, T., Kokkalas, S., 2001. Stress and deformation patterns in the Aegean region. In: Dunne, W.M., Stewart I.S., Turner, J.P. (Eds.), Paul Hancock Memorial Issue. Journal of Structural Geology 23, pp. 455–472.

Ego, F., Sebrier, M., 1996. The Ecuadorian Inter-Andean valley; a major and complex restraining bend and compressive graben since late Miocene time. Annales Tectonicæ 10, 31–59.

Etchecopar, A., Vasseur, G., Daignieres, M., 1981. An inverse problem in the microtectonics for the determination of stress tensors from fault striation analysis. Journal of Structural Geology 3, 51–65.

Fernández, C., Nuez, J., Casillas, R., Navarro, E.G., 2002. Stress field associated with the growth of a large shield volcano (La Palma, Canary Islands). Tectonics 21, 13–18.

Ferrari, L., López-Martínez, M., Rosas-Elguera, J., 2002. Ignimbrite flare-up and deformation in the southern Sierra Madre Occidental, western Mexico: implications for the late subduction history of the Farallon plate. Tectonics 21, 17–24.

Gayer, R., Hathaway, T., Nemcok, M., 1998. Transpressionally driven rotation in the external orogenic zones of the Western Carpathians and the SW British Variscides. In: Holdsworth, R., Strachan, R.A., Dewey, J.F. (Eds.), Continental Transpressional and Translational Tectonics. Geological Society, London, Special Publication 135, pp. 253–266.

Geoffroy, L.F., Bergerat, F., Angelier, J., 1996. Brittle tectonism in relation to the Palaeogene evolution of the Thulean/NE Atlantic domain: a study in Ulster. Geological Journal 31, 259–269.

Ghisetti, F., 2000. Slip partitioning and deformation cycles close to major faults in southern California: evidence from small-scale faults. Tectonics 19, 25–43.

González-Casado, J.M., López-Martínez, J., Durán, J.J., 1999. Active tectonics and morphostructure at the northern margin of the Central Bransfield Basin, Hurd Peninsula, Livingston Island (South Shetland Islands). Antarctic Science 11(3), 323–331.

González-Casado, J.M., Giner-Robles, J., López-Martínez, J., 2000. The Bransfield Basin, Antarctic Peninsula: not a 'normal' back-arc basin. Geology 28, 1043–1046.

Gudmundsson, A., Bergerat, F., Angelier, J., Villemin, T., 1992. Extensional tectonics of southwest Iceland. Bulletin de la Société Géologique de France 16, 1555–1573.

Hardcastle, K.C., 1989. Possible palaeostress tensor configurations derived from fault-slip data in Eastern Vermont and New Hampshire. Tectonics 8, 265–284.

Hippolyte, J.C., 2002. Geodynamics of Dobrogea (Romania): new constraints on the evolution of the Tornquist–Teisseyre Line, the Black Sea and the Carpathians. Tectonophysics 357, 33–53.

Hippolyte, J.C., Angelier, J., Roure, F., Casero, P., 1994. Piggyback basin development and thrust belt evolution; structural and palaeostress analyses of Plio-Quaternary basins in the Southern Apennines. Journal of Structural Geology 16, 159–173.

Hippolyte, J.C., Angelier, J., Barrier, E., 1995. Compressional and extensional tectonics in an arc system; example of the Southern Apennines. Journal of Structural Geology 17, 1725–1740.

Hippolyte, J.C., Badescu, D., Constantin, P., 1999. Evolution of the transport direction of the Carpathian belt during its collision with the east European Platform. Tectonics 18, 1120–1138.

Homberg, J.C., Angelier, J., Bergerat, F., Lacombe, O., 1997. Characterization of stress perturbations near major fault zones; insights from 2-D distinct-element numerical modelling and field studies (Jura Mountains). Journal of Structural Geology 19, 703–718.

Huismans, R.S., Bertotti, G., 2002. The Transylvanian basin, transfer zone between coeval extending and contracting regions: inferences on the relative importance of slab pull and rift push in arc-back arc systems. Tectonics 21, 2–20.

Hurst, S.D., Moores, E.M., Varga, R.J., 1994. Structural and geophysical expression of the Solea Graben, Troodos Ophiolite, Cyprus. Tectonics 13, 139–156.

Kaymakci, N., White, S.H., Vandijk, P.M., 2003. Kinematic and structural development of the Qankiri Basin (Central Anatolia, Turkey): a paleostress inversion study. Tectonophysics 364, 85–113.

Keele, R.A., Wright, J.V., 1998. Analysis of some fault striations in the Proterozoic southern McArthur Basin, northern Territory, with reference to pre- and post-Roper Group stress fields. Australian Journal of Earth Sciences 45, 51–61.

Kleinspehn, L., 1989. Paleostress stratigraphy; a new technique for analyzing tectonic control on sedimentary basin subsidence. Geology 17, 253–256.

Lacombe, O., Bergues, J., Angelier, J., Laurent, P., 1991. Quantification des paleocontraintes a l'aide des macles de la calcite; l'exemple de la compression pyreneo-provencale au front de la Montagne Sainte-Victoire (Provence). Comptes Rendus de l'Academie des Sciences, Serie 2, France 313(10), 1187–1194.

Lacombe, O., Angelier, J., Byrne, D., Dupin, J.M., 1993. Eocene–Oligocene tectonics and kinematics of the Rhine-Saone continental transform zone (Eastern France). Tectonics 12, 874–888.

Lacombe, O., Angelier, J., Rocher, M., Bergues, J., Deffontaines, B., Chu, H.T., Hu, J.C., Lee, J.C., 1996. Contraintes et plissement au front d'une chaine de collision; l'exemple des calcaires récifaux pliocenes de Yutengping (Taiwan). Bulletin de la Société Géologique de France 167, 361–374.

Lamarche, J., Bergerat, F., Lewandowski, M., Mansy, J.L., Świdorwska, J., Wieczoreck, J., 2002. Variscan to Alpine heterogeneous palaeo-stress field above a major Paleozoic suture in the Carpathian foreland (southeastern Poland). Tectonophysics 357, 55–80.

Lavenu, A., Noblet, C., Winter, T., 1995. Neogene ongoing tectonics in the southern Ecuadorian Andes; analysis of the evolution of the stress field. Journal of Structural Geology 17, 47–58.

Lepvrier, C., Leparmentier, F., Seland, R., 1989. Upper Palaeozoic faulting regimes in Bjornoya (Svalbard, Norway). Bulletin de la Société Géologique de France 5, 411–416.

Lepvrier, C., Fournier, M., Berard, T., Roger, J., 2002. Cenozoic extension in coastal Dhofar (southern Oman): implications on the oblique rifting of the Gulf of Aden. Tectonophysics 357, 279–293.

Lewis, C.L., Stock, J.M., 1998. Late Miocene to Recent transtensional tectonics in the Sierra San Fermín, northeastern Baja California, Mexico. Journal of Structural Geology 20, 1043–1063.

Mercier, J.L., Carey-Gailhardis, E., Mouyaris, N., Simeakis, K., Roundoyannis, T., Anghelidhis, C., 1983. Structural analysis of Recent and active faults and regional state of stress in the epicentral area of the 1978 Thessaloniki earthquakes (northern Greece). Tectonics 2, 577–600.

Mercier, J.L., Armijo, R., Tapponnier, P., Carey-Gailhardis, E., Lin, H.T., 1987. Change from Late Tertiary compression to Quaternary extension in Southern Tibet during the India–Asia collision. Tectonics 6, 275–304.

Mounthereau, F., Lacombe, O., Deffontaines, B., Angelier, J., Chu, H.T., Lee, C.T., 1999. Quaternary transfer faulting and belt front deformation at Pakuashan (western Taiwan). Tectonics 18, 215–230.

Nemcok, M., Gayer, R.A., 1996. Modelling palaeostress magnitude and age in extensional basins; a case study from the Mesozoic Bristol Channel basin, U.K. Journal of Structural Geology 18, 1301–1314.

Nemcok, M., Gayer, R., Miliorizos, M., 1995. Structural analysis of the inverted Bristol Channel basin; implications for the geometry and timing of fracture porosity. In: Buchanan, J.G. (Ed.), Basin Inversion. Geological Society, London, Special Publications 88, pp. 355–392.

Nemcok, M., Henk, A., Gayer, R.A., Vandycke, S., Hathaway, T., 2002. Strike-slip fault bridge fluid pumping mechanism: insight from field-based palaeostress analysis and numerical modelling. Journal of Structural Geology 24, 1885–1901.

Nieto-Samaniego, A.F., Ferrari, L., Alaniz-Alvarez, S.A., Labarthe-Hernandez, G., Rosas-Elguera, J., 1999. Variation of Cenozoic extension and volcanism across the southern Sierra Madre Occidental volcanic province, Mexico. Bulletin of the Geological Society America 111, 347–363.

Över, S., Bellier, O., Poisson, A., Adrieux, J., 1997. Late Cenozoic stress state changes along the central North Anatolian Fault Zone (Turkey). Annales Tectonicæ 11, 75–101.

Poisson, A., Lukowski, P., 1990. The Fortuna basin: a piggyback basin in the eastern Betic Cordilleras (SE Spain). Annales Tectonicæ, 4, 52–67.

Quinif, Y., Vandycke, S., Vergari, A., 1997. Chronologie et causalité entre tectonique et karstification L'exemple de paléokarsts crétacés du Hainaut (Belgique). Bulletin de la Société Géologique de France 168, 423–436.

Ratschbacher, L., Linzer, H.G., Moser, F., Strusievicz, R.O., Bedelean, H., Har, N., Mogos, P.A., 1993. Cretaceous to Miocene thrusting and wrenching along the Central Carpathians due to a corner effect during collision and orocline formation. Tectonics 12, 855–858.

Rebai, S., 1993. Recent tectonics in northern Tunisia; coexistence of compressive and extensional structures. Annales Tectonicæ 7, 129–141.

Rocher, M., Lacombe, O., Angelier, J., Deffontaines, B., Verdier, F., 2000. Cenozoic folding and faulting in the South Aquitaine Basin (France); insights from combined structural and paleostress analysis. Journal of Structural Geology 22, 627–645.

Rocher, M., Tremblay, A., Lavoie, D., 2003. Brittle fault evolution of the Montreal area (St. Lawrence lowlands, Canada): rift-related structural inheritance and tectonism approached by paleostress analysis. Geological Magazine 140, 157–172.

Rossetti, F., Faccenna, C., Goffé, B., Moiné, P., Agentieri, A., Funiciello, R., Mattei, M., 2001. Alpine structural and metamorphic signature of the Sila Piccola Massif nappe stack (Calabria, Italy); insights for the tectonic evolution of the Calabrian Arc. Tectonics 20, 112–133.

Saintot, A., Angelier, J., 2000. Plio-Quaternary paleostress regimes and relation to structural development in the Kertch–Taman peninsulas (Ukraine and Russia). Journal of Structural Geology 22, 1049–1064.

Saintot, A., Angelier, J., 2002. Tectonic paleostress fields and structural evolution on the NW Caucasus fold-and-thrust belt from Late Cretaceous to Tertiary. Tectonophysics 357, 1–31.

Sebriér, M., Mercier, J.L., Macharé, J., Bonnot, D., Cabrera, J., Blanc, J.L., 1988. The state of stress in an overriding plate situated above a flat slab: The Andes of Central Peru. Tectonics 7, 895–928.

Sintubin, M., Nefly, M., Rijpens, J., Van Zegbroek, B., 1997. Faulting history at the eastern termination of the High Atlas Fault. (Western High Atlas, Morocco). Geologie en Mijnbouw 76, 187–195.

Sperner, B., Ratschbacher, L., Ott, R., 1993. Fault-striae analysis: a TURBO PASCAL package for graphical presentation and reduced stress tensor calculation. Computers and Geosciences 19, 1361–1388.

Srivastava, D.C., Sahay, A., 2003. Brittle tectonics and porefluid conditions in the evolution of the Great Boundary Fault around Chittarugrah, Northwestern India. Journal of Structural Geology 25, 1713–1733.

Srivastava, D.C., Lisle, R.J., Vandycke, S., 1995. Shear zones as a new type of paleostress indicator. Journal of Structural Geology 17, 663–676.

Strecker, M.R., Frisch, W., Hamburger, M.W., Ratschbacher, L., Semiletkin, S., Zamoruyev, A., Sturchio, N., 1995. Quaternary deformation in the eastern Pamirs, Tadzhikistan and Kyrgyzstan. Tectonics 14, 1061–1079.

Suter, M., Quintero, L.O., Lopez, M.M., Aguirre, D.G., Farrar, E., 1995. The Acambay Graben; active intra-arc

extension in the Trans-Mexican volcanic belt, Mexico. Tectonics 14, 1245–1262.
Temiz, H., Poisson, A., Andrieux, J., Barka, A., 1997. Kinematics of the Plio-Quaternary Burdur-Dinar cross-fault system in SW Anatolia (Turkey). Annales Tectonicae 11, 102–113.
Titus, S.J., Fossen, H., Pedersen, R.B., Vigneresse, J.L., Tikoff, B., 2002. Pull-apart formation and strike-slip partitioning in an obliquely divergent setting, Leka Ophiolite, Norway. Tectonophysics 354, 101–119.
Vandycke, S., 2002. Palaeostress records in Cretaceous Formations in the NW Europe: extensional and strike-slip events in relationships with Cretaceous–Tertiary inversion tectonics. Tectonophysics 357, 119–136.
Vandycke, S., Bergerat, F., 1989. Analyse microtectonique des deformations cassantes dans le Bassin de Mons; reconstruction des paleo-champs de contrainte au Cretace–Tertiaire. In: Dupuis, C., Camelbeeck, T. (Eds.), Tectonique actuelle et recente en Belgique, a propos des tremblements de terre en Hainaut; colloque. Annales de la Societe Geologique de Belgique 112, pp. 469–478.
Vandycke, S., Bergerat, F., 1992. Tectonique de failles et paléo-contraintes dans les formations crétacées du Boulonnais (France). Implications géodynamiques. Bulletin de la Société Géologique de France 163, 553–560.
Vandycke, S., Bergerat, F., 2001. Brittle tectonic structures and palaeostress analysis in the Isle of Wight, Wessex Basin, southern U.K. In: Dunne, W.M., Stewart, I.S., Turner, J.P. (Eds.), Paul Hancock Memorial Issue. Journal of Structural Geology 23, pp. 393–406.
Vandycke, S., Bergerat, F., Dupuis, C., 1987. Paleo-contraintes a la limite Cretace–Tertiaire dans le Bassin de Mons (Belgique); implications cinematiques relations avec la zone de cisaillement Nord-Artois. Comptes Rendus de l'Academie des Sciences, Serie 2, 307, 303–309.
Varga, R.J., 1991. Modes of extension at oceanic spreading centers; evidence from the Solea Graben, Troodos Ophiolite, Cyprus. Journal of Structural Geology 13, 517–537.
Varga, R.J., 1993. Rocky Mountain foreland uplifts; products of a rotating stress field or strain partitioning. Geology 21, 1115–1118.
Villemin, T., Bergerat, F., Angelier, J., Christian, L., 1994. Brittle deformation and fracture patterns on oceanic rift shoulders; the Esja Peninsula, SW Iceland. Journal of Structural Geology 16, 1641–1654.
Vrabec, M., Car, J., Veber, I., 1999. Kinematics of the Sostanj Fault in the Velenje Basin area; insights from subsurface data and paleostress analysis. RMZ Materials and Geoenvironment 46, 623–634.
Wise, D.U., Obi, C.M., 1992. Laramide basement deformation in an evolving stress field, Bighorn Mountain front, Five Springs area, Wyoming. AAPG Bulletin, 76, 1586–1600.
Zanchi, A., 1994. The opening of the Gulf of California near Loreto, Baja California, Mexico; from basin and range extension to transtensional tectonics. Journal of Structural Geology 16, 1619–1639.
Zanchi A., Crosta, G.B., Darkal, A.N., 2002. Paleostress analyses in NW Syria: constraints on the Cenozoic evolution of the northwestern margin of the Arabian plate. Tectonophysics 357, 255–278.

References

Aleksandrowski, P., 1985. Graphical determination of principal stress directions for slickenside lineation populations; an attempt to modify Arthaud's method. Journal of Structural Geology 7, 73–82.
Anderson, E.M., 1951. The Dynamics of Faulting. Oliver & Boy, Edinburgh. 206pp.
Angelier, J., 1975. Sur l'analyse de mesures recueillies sans des sites faillés: l'utilité d'une confrontation entre les méthodes dynamiques et cinématiques. Comptes Rendus de l'Academie des Sciences, Paris D281, 1805–1808.
Angelier, J., 1984. Tectonic analysis of fault slip data sets. Journal of Geophysical Research B89, 5835–5848.
Angelier, J., 1994. Fault slip analysis and palaeostress reconstruction. In: Hancock, P.L. (Ed.), Continental Deformation. Pergamon Press, New York, pp. 53–100.
Arthaud, F., 1970. Méthode de détermination graphique des directions de raccourcissement, d'allongement et intermédiaire d'une population de failles. Bulletin de la Société Géologique de France 11, 729–737.
Bergerat, F., 1987. Stress fields in the European Platform at the time of Africa–Eurasia Collision. Tectonics 6, 99–132.
Bishop, A.W., 1966. The strength of soils as engineering materials. Géotechnique 16, 91–128.
Bott, M.H.P., 1959. The mechanisms of oblique slip faulting. Geological Magazine 96, 109–117.
Byerlee, J.D., 1978. Friction of rocks. Pure and Applied Geophysics 116, 615–626.
Carey, E., Brunier, B., 1974. Numerical analysis of an elementary mechanical model applied to the study of a population of faults. Comptes Rendus de l'Academie des Sciences, Paris Serie D 279, 891–894.
Carey, E., Mercier, J.L., 1987. A numerical method of determining the state of stress using focal mechanisms of earthquake populations: applications to Tibetan teleseisms and microseismicity of S Peru. Earth and Planetary Science Letters 82, 165–179.
Carmichael, R.S., 1982. Handbook of Physical Properties of Rocks, Vol. 2. CRC Press, Boca Raton. 345pp.
Cheeney, R.F., 1983. Statistical Methods in Geology. George Allen & Unwin, London. 169pp.
Etchecopar, A., Vasseur, G., Daignieres, M., 1981. An inverse problem in microtectonics for the determination of stress tensors from fault striation analysis. Journal of Structural Geology 3, 51–65.
Fry, N., 1992. Stress ratio determinations from striated faults; a spherical plot for cases of near-vertical principal stress. Journal of Structural Geology 14, 1121–1131.
Hardcastle, K.C., Hills, L.S., 1991. Brute3 and Select—QuickBasic 4 programs for determination of stress tensor configurations and separation of heterogeneous populations of fault-slip data. Computers & Geosciences 17, 23–43.
Lisle, R.J., 1979. The representation and calculation of the deviatoric component of the geological stress tensor. Journal of Structural Geology 1, 317–321.
Mercier, J.L., Armijo, R., Tapponnier, P., Carey-Gailhardis, E., Lin, H.T., 1987. Change from Late Tertiary compression to Quaternary extension in Southern Tibet during the India–Asia collision. Tectonics 6, 275–304.
Nádai, A., 1950. Theory of Flow and Fracture of Solids, Vol. 1. McGraw-Hill, New York.
Orife, T.O., 2001. The application of palaeostress techniques to analysis of subsurface data. Unpublished PhD thesis, Cardiff University.

Orife, T., Lisle, R.J., 2003. Numerical processing of palaeostress results. Journal of Structural Geology 25, 949–957.

Paterson, M.S., 1978. Experimental Rock Deformation: the Brittle Field. Springer Verlag, Berlin. 254pp.

Ramsay, J.G., 1967. Folding and Fracturing of Rocks. McGraw-Hill, New York.

Ramsay, J.G., Lisle, R.J., 2000. The Techniques of Modern Structural Geology; Vol. 3. Applications of Continuum Mechanics in Structural Geology. Academic Press, London, pp. 701–1061.

Ramsay, J.G., Wood, D.S., 1973. The geometric effects of volume change during deformation processes. Tectonophysics 16, 263–277.

Reinecker, J., Heidbach, O., Tingay, M., Connolly, P., Müller, B., 2004. The 2004 release of the World Stress Map 2004 (available online at www.world-stress-map.org).

Sato, K., Yamaji, A., 2006. Uniform distribution of points on a hypersphere for improving the resolution of stress tensor inversion. Journal of Structural Geology, this issue, doi: 10.1016/j.jsg.2006.03.007.

Simón-Gómez, J.L., 1986. Analysis of a gradual change in stress regime (example from the eastern Iberian Chain, Spain). Tectonophysics 124, 37–53.

Sperner, B., Ratschbacher, L., Ott, R., 1993. Fault striae analysis: a Turbo Pascal program package for graphical representation and reduced stress tensor calculation. Computers & Geosciences 19, 1362–1388.

Wallace, R.E., 1951. Geometry of shearing stress and relation to faulting. Journal of Geology 59, 118–130.

Zoback, M.L., 1992. First- and second-order patterns of stress in the lithosphere: the World Stress Map Project. Journal of Geophysical Research 97 (B8), 11,703–11,728.

Zoback, M.L., Zoback, M.D., Adams, J., Assumpcao, M., Bell, S., Bergman, E.A., Bluemling, P., Brereton, N.R., Denham, D., Ding, J., Fuchs, K., Gay, N., Gregersen, S., Gupta, H.K., Gvishiani, A., Jacob, K., Klein, R., Knoll, P., Magee, M., Mercier, J.L., Mueller, B.C., Paquin, C., Rajendran, K., Stephansson, O., Suarez, G., Suter, M., Udias, A., Xu, Z.H., Zhizin, M., 1989. Global patterns of tectonic stress. Nature 341, 291–299.